JOURNAL OF VIROLOGY, Dec. 2008, p. 12374–12383 Vol. 82, No. 24
0022-538X/08/$08.00+0 doi:10.1128/JVI.00985-08

Ross River Virus Envelope Glycans Contribute to Type I Interferon Production in Myeloid Dendritic Cells[▽]

Reed S. Shabman, Kristin M. Rogers, and Mark T. Heise*

Department of Genetics, Department of Microbiology and Immunology, and Carolina Vaccine Institute, University of North Carolina—Chapel Hill, Chapel Hill, North Carolina 27599

Received 12 May 2008/Accepted 25 September 2008

Alphaviruses are mosquito-transmitted viruses that cause significant human disease, and understanding how these pathogens successfully transition from the mosquito vector to the vertebrate host is an important area of research. Previous studies demonstrated that mosquito and mammalian-cell-derived alphaviruses differentially induce type I interferons (alpha/beta interferon [IFN-α/β]) in myeloid dendritic cells (mDCs), where the mosquito cell-derived virus is a poor inducer of IFN-α/β compared to the mammalian-cell-derived virus. Furthermore, the reduced IFN-α/β induction by the mosquito cell-derived virus is attributed to differential N-linked glycosylation (29). To further evaluate the role of viral envelope glycans in regulating the IFN-α/β response, studies were performed to assess whether the mosquito cell-derived virus actively inhibits IFN-α/β induction or is simply a poor inducer of IFN-α/β. Coinfection studies using mammalian- and mosquito cell-derived Ross River virus (mam-RRV and mos-RRV, respectively) indicated that mos-RRV was unable to suppress IFN-α/β induction by mam-RRV in mDC cultures. Additionally, a panel of mutant viruses lacking either individual or multiple N-linked glycosylation sites was used to demonstrate that N-linked glycans were essential for high-level IFN-α/β induction by the mammalian-cell-derived virus. These results suggest that the failure of the mosquito cell-derived virus to induce IFN-α/β is due to a lack of complex carbohydrates on the virion rather than the active suppression of the DC antiviral response.

Mosquito-borne viruses, which include toga-, flavi-, and bunyaviruses, are a significant and emerging cause of human diseases ranging from hemorrhagic fever to encephalitis and arthritis (8, 12, 24). Though the mechanisms by which these viruses cause disease are diverse, a common and essential step in the viral life cycle is successful transition from the mosquito vector to the vertebrate host. For many of these viruses, Langerhans cells and/or dermal myeloid dendritic cells (mDCs) appear to be an early target of viral replication following transmission from the mosquito vector (21, 36). mDCs are professional antigen-presenting cells that rapidly respond to viruses in the absence of viral replication and are capable of producing type I interferons (alpha/beta interferon [IFN-α/β]) to high levels (7, 10). Understanding how these viruses target and successfully establish infection in DCs is an important and rapidly developing area of research.

Several reports indicate that viral N-linked glycans are major mediators of DC tropism, with the presence of high-mannose-content N-linked glycans on mosquito cell-derived Sindbis virus and West Nile virus (WNV) enhancing the infection of mDCs due to interactions with the mannose binding C-type lectin receptor (CLR) DC-SIGN (5, 16). These results suggest that CLRs act as attachment receptors to enhance the infection of DCs and macrophages, though it is likely that other molecules act as entry receptors. In addition to enhancing infection, high-mannose N-linked glycans on mosquito cell-derived virions are linked to poor IFN-α/β induction in mDCs (29) and plasmacytoid DC cultures (31). Furthermore, mosquito cell-derived WNV has been shown previously to actively inhibit poly(I-C)-induced IFN-α/β responses in macrophages (1). Virus inhibition of the innate immune response is not limited to arthropod-borne viruses, since high-mannose N-linked glycans on the gp120 molecule of human immunodeficiency virus suppress mDC responses following DC-SIGN binding (30).

While a growing body of evidence suggests that high-mannose N-linked glycans negatively regulate antiviral responses, the findings of some studies indicate that viral glycoproteins either assembled as virus-like particles (VLPs) or fixed on the surfaces of infected cells can stimulate type I IFN through interactions with lectins (15). Charley et al. demonstrated that complex, but not high-mannose, N-linked glycans on the transmissible gastroenteritis virus M protein are responsible for IFN induction in porcine peripheral blood mononuclear cells (4). Transmissible gastroenteritis virus mutants lacking N-linked glycan sites are poor inducers of IFN-α (19). Additional studies have demonstrated that both the highly ordered structure of an assembled VLP (2) and the glycan linkage (N-linked but not O-linked glycans) are critical for robust IFN-α/β production (6). Similar results obtained with influenza virus demonstrated a requirement for interactions between sialic acid on the virus particle and mouse spleen cells for IFN-α/β production (23). Finally, Ebola VLP stimulation of human mDCs requires the heavily glycosylated mucin domain (22). Taken together, these data suggest that interactions between lectin receptors and viral N-linked glycans are capable of both suppressing and activating antiviral responses in IFN-producing cells.

Previous work from our laboratory demonstrated that mosquito cell-derived alphaviruses are poor inducers of IFN-α/β and that mammalian-cell-derived alphaviruses induce robust

* Corresponding author. Mailing address: Carolina Vaccine Institute, University of North Carolina, Chapel Hill, NC 27599. Phone: (919) 843-1492. Fax: (919) 843-6924. E-mail: heisem@med.unc.edu.

▽ Published ahead of print on 15 October 2008.

IFN-α/β responses in mDCs (29). This effect is regulated at least partly by the glycosylation of the virion, and high-mannose glycans are poor inducers of IFN-α/β, while virus with complex sugars induces robust IFN-α/β responses. In this study, Ross River virus (RRV) was used to assess whether IFN-α/β induction differences represented active suppression or if complex sugars were required for efficient IFN-α/β induction in mDCs. A panel of RRV N-linked-glycan-deficient viruses was developed and compared to wild-type RRV for infectivity and IFN-α/β induction following mDC infection. These studies showed that the N-linked glycans on the E2 glycoprotein of mammalian-cell-derived RRV (mam-RRV) were required for robust IFN-α/β induction in mDC cultures.

MATERIALS AND METHODS

Recombinant virus design. RRV (T48 strain) was kindly provided by Richard Kuhn, Purdue University. The pRR64 plasmid, which carries the entire cDNA genome of RRV (17), was used to generate recombinant viruses containing either single or multiple N-linked glycosylation site mutations on the E2 and E1 glycoproteins. Asparagine-to-glutamine mutations at each glycosylation site were introduced by standard site-directed mutagenesis at amino acids 200 and 262 in the E2 glycoprotein and amino acid 141 in the E1 glycoprotein. All mutant clones were sequenced, and mutated DNA fragments were subcloned into the backbone of both RRV and RRV expressing the green fluorescent protein (GFP) gene between the unique ApaI site (located in the region encoding NSP4, at nucleotide 6746) and the unique XmaI site (located in the region encoding E1, at nucleotide 10693).

Generation of virus stocks and plaque assays. Plasmid pRR64 was used to generate recombinant virus stocks as described previously (29). Briefly, pRR64 was linearized by SacI digestion, full-length RNA transcripts were generated by in vitro transcription (Ambion), and RNA was introduced into baby hamster kidney 21 (BHK-21) cells (ATCC CCL-10) by electroporation. Twenty-four hours postelectroporation, mam-RRV-containing supernatants were harvested and clarified via centrifugation at 3,000 rpm in a Sorvall Legend RT centrifuge. Clarified supernatants were either aliquoted or concentrated through a 20% (wt/vol) sucrose cushion at 72,000 × *g*, and virus was resuspended in phosphate-buffered saline supplemented with 1% fetal bovine serum (FBS), calcium, and magnesium. To generate mosquito cell-derived RRV (mos-RRV), mam-RRV was passaged at a multiplicity of infection (MOI) of 0.1 in C6/36 *Aedes albopictus* cells (ATCC CRL-1660). After a 1-h attachment period, cells were washed twice to remove unattached virus. At 18 to 24 h postinfection (hpi), supernatant was harvested and concentrated in the same manner as that described above for mam-RRV. Titers of both mam-RRV and mos-RRV on BHK-21 cells were determined by a standard plaque assay. Briefly, BHK-21 cells were seeded into 60-mm dishes and infected with serial 10-fold dilutions of virus stocks for 1 h. Cell monolayers were overlaid with 0.4% immunodiffusion agarose (MP Biomedicals) in medium for 40 to 44 h and then stained with neutral red (Sigma). Plaques were counted to determine the number of PFU per milliliter of each virus stock.

BHK-21 cells were grown in minimal essential medium alpha medium (Gibco) supplemented with 10% FBS, 10% tryptose phosphate, L-glutamine, penicillin, and streptomycin. C6/36 cells were grown in minimal essential medium containing Earle's salts, FBS, penicillin, streptomycin, and nonessential amino acids.

UV inactivation. Both mock and virus samples were subjected to 254 nm of shortwave UV light at a distance of 5 cm from the source (Mineralight lamp; model no. UVG-54). Virus inactivation was confirmed by both the loss of GFP expression from a second 26S subgenomic promoter following mDC infection and the loss of plaque formation on BHK-21 cells.

Bone marrow mDC cultures and infection conditions. Bone marrow-derived DCs were prepared as described previously (28). Briefly, the tibia and femur of a 129 Sv/Ev mouse were removed, and bone marrow was isolated. Red blood cells were lysed, and the remaining cells were differentiated in granulocyte-macrophage colony-stimulating factor and interleukin-4 (Peprotech) for 7 days in ultralow-cluster six-well plates (Costar). Bone marrow-derived DCs were cultured in RPMI 1640 supplemented with 10% FBS, L-glutamine, penicillin and streptomycin, and 2-mercaptoethanol. The status of immature DCs was confirmed as described previously (28). The levels of surface expression of CD11c, CD11b, and major histocompatibility complex class II molecules were quantified, and the absence of B220 was verified by fluorescence-activated cell sorting. Cultures were routinely ≥90% CD11c positive, ≥95% CD11b positive, and B220 negative, which is consistent with an mDC phenotype (29). At 7 days postisolation, cells were either frozen or used for infectivity studies. Infections were initiated with a 0.2-ml total volume for 2 h, and then 0.5 ml of medium was added to each well of a 24-well plate. At 12 hpi, cells were harvested and GFP expression was quantified by flow cytometry.

Type I IFN (IFN-α/β) bioassay. IFN-α/β levels in cell culture supernatants were measured by an IFN bioassay as described previously (29, 35). L929 mouse fibroblasts (ATCC CCL-1) were seeded into 96-well plates and grown in the same medium as BHK-21 cells. Samples were acidified to a pH of 2.0 for 24 h and then neutralized to pH 7.4. Additional virus inactivation by UV light (as described above) was performed prior to titration by twofold serial dilutions across the plate. Twenty-four hours later, encephalomyocarditis virus was added to each well at an MOI of 5. At 18 to 24 hpi, 3-(4,5-dimethyl-2-thiazolyl)-2,5-diphenyl-2H-tetrazolium bromide (MTT; Sigma) was used to assess the viability in each well. The MTT product produced by viable cells was dissolved in isopropanol–0.4% HCl and quantified by absorbance readings on a microplate reader at 570 nm. Each plate contained an IFN-β standard (Chemicon or R&D Systems) which was used to determine the number of international units of IFN-α/β per milliliter of the unknown samples. Alternatively, IFN-β levels were quantified using a mouse IFN-β enzyme-linked immunosorbent assay (ELISA) kit (PBL Biomedical Laboratories, Piscataway, NJ). ELISAs were performed per the manufacturer's instructions except that the IFN-β standard was diluted in RPMI 1640 supplemented with 10% FBS, L-glutamine, penicillin and streptomycin, and 2-mercaptoethanol instead of the sample diluent provided in the kit.

Single-step and multistep growth curve analyses. BHK-21 cells were seeded into 24-well plates and infected with wild-type RRV and each mutant virus for 1 h at an MOI of 5 or 0.01. Virus inocula were removed, and cells were washed to remove unbound virus. At 1, 3, 6, 9, 12, 24, and 30 hpi, 100-μl aliquots were removed and virus titers were determined by plaque assays as described above except that assays were performed with six-well plates.

Real-time PCR. For RRV genome analysis, Sybr green primers described previously (29) or a TaqMan primer-probe set (designed with the Primer Express software) specific for the NSP3 region of RRV was used. The primer pairs were used to determine the ratio of RRV genomes to PFU for mam-RRV and mos-RRV stocks, and independent analyses of several stocks gave similar results. The primer and probe sequences for the TaqMan primer-probe set were as follows: forward primer, 5′-CCGTGGCGGGTATTATCAAT-3′; reverse primer, 5′-AACACTCCCGTCGACAACAGA-3′; and probe, 5′-ATTAAGAGTGTAG CCATCC-3′. Purified virion RNA was isolated with the 96-well MagMax viral RNA extraction kit (Ambion). Virion RNA was reverse transcribed using mouse murine leukemia virus reverse transcriptase (Invitrogen), and a dilution of cDNA was used for quantitative real-time PCR. A DNA standard curve for the RRV genome was generated to ensure optimal primer-probe efficiency and to assign relative genome numbers to directly compare each sample. The data obtained from the real-time PCR assay were normalized to the number of PFU from the same virus stock to generate a relative genome number-to-PFU ratio.

Assays of specific infectivity of RNA. RNA from each RRV glycoprotein mutant virus was transcribed from the corresponding mutant pRR64 plasmid. The DNA template was digested with DNase, and RNA was precipitated with LiCl and quantified by absorbance at 260 nm. BHK-21 cells in 60-mm dishes were transfected with serial dilutions of RNA for 15 min by using Lipofectamine 2000 (Invitrogen), and cells were overlaid with minimal essential medium alpha medium and 0.4% immunodiffusion agarose. Forty hours posttransfection, dishes were stained with neutral red, plaques were enumerated, and the number of PFU per microgram of RNA was determined.

Endoglycosidase digestions and Western blotting. Equivalent numbers of PFU from each of the purified viruses produced in either BHK-21 or C6/36 cells were either mock digested or digested with PNGase or endo H (New England Biolabs) overnight according to the manufacturer's protocol. Equal volumes of each of the digested virion preparations were analyzed on a sodium dodecyl sulfate (SDS)–10% polyacrylamide gel electrophoresis (PAGE) gel and then subjected to Western blot analysis using an anti-RRV mouse hyperimmune ascites fluid (ATCC VR-1246AF). Protein bands were visualized by ECL Plus (Amersham) immunofluorescence and developed with film (Amersham Hyperfilm ECL).

Statistics. All relevant groups were compared using a one-way analysis of variance (ANOVA) or an unpaired Student *t* test, where indicated, with GraphPad InStat software, version 3.06.

RESULTS

Mos-RRV does not actively suppress the IFN-α/β response in mDCs induced by mam-RRV. Previous studies from our group demonstrated that mos-RRV infects mDCs more efficiently than mammal-derived virus but that mam-RRV is a more potent inducer of type I IFN production than mos-RRV (29). This effect is mediated at least partly by differences in viral glycosylation, since both mosquito and mammalian-cell-derived viruses grown in cells that produce only high-mannose N-linked glycans are poor IFN inducers (29). The findings of studies by other groups demonstrated that N-linked glycans from C6/36-derived WNV can suppress IFN-α/β induction in response to double-stranded RNA stimulation of macrophages (1) and that high-mannose residues on human immunodeficiency virus gp120 have immunosuppressive effects on DCs (30). Therefore, coinfection studies using mam-RRV and mos-RRV were performed to determine whether the poor IFN induction by mos-RRV reflected active inhibition of type I IFN induction.

Consistent with the results of previous studies (29), mam-RRV induced IFN-α/β in mDCs to higher levels than mos-RRV, even when a fivefold excess of mos-RRV was used (444.0 IU of IFN-α/β per ml for mam-RRV at an MOI of 10 versus 96.3 IU per ml for mos-RRV at an MOI of 50) (Fig. 1A). We hypothesized that if mos-RRV was actively suppressing IFN-α/β induction in mDCs, coinfection with mos-RRV and mam-RRV would result in the loss of high-level IFN-α/β induction. However, coinfection with a fivefold excess of mos-RRV relative to mam-RRV had no effect on mam-RRV-mediated IFN-α/β induction (yielding 419.6 IU/ml) (Fig. 1A). These results were confirmed with UV-inactivated RRV. We have previously shown that UV-inactivated mam-RRV induces IFN-α/β and that UV-inactivated mos-RRV fails to induce (29), thereby allowing us to evaluate the effects of mosquito cell-derived virus independently of productive viral replication. For these studies, we UV inactivated RRV over a time course and determined a dose of UV light that resulted in the loss of the ability of RRV to infect mDCs and form plaque on BHK cells but still allowed the virus to induce IFN-α/β on DCs (data not shown). As shown in Fig. 1B, UV-treated mos-RRV at a fivefold excess was still a poor inducer of IFN-α/β compared to UV-treated mam-RRV (16.6 IU/ml for mos-RRV at an MOI of 50 versus 197.6 IU/ml for mam-RRV at an MOI of 10). Coinfection with UV-inactivated mam-RRV at an MOI of 10 and UV-inactivated mos-RRV at an MOI of 50 had no effect on IFN-α/β induction (yielding 186.4 IU/ml). Though these results do not absolutely rule out the active inhibition of IFN-α/β induction by mos-RRV, they do strongly suggest that mos-RRV is unable to induce a general block of IFN-α/β induction in mDCs.

Generation and characterization of RRV glycan mutants. The coinfection studies suggested that mos-RRV did not inhibit mam-RRV IFN-α/β induction in murine mDCs. To further evaluate the role of viral N-linked glycans in this process, we generated a panel of viruses lacking one or more of the three viral envelope N-linked glycosylation sites. Amino acid changes from asparagine (N) to glutamine (Q) were introduced at each glycosylation site in the T48 infectious clone of RRV (E2 amino acids 200 and 262 and E1 amino acid 141) (17, 39) by site-directed mutagenesis, and changes were confirmed by sequence analysis. A diagram of each mutant virus generated is shown in Fig. 2A.

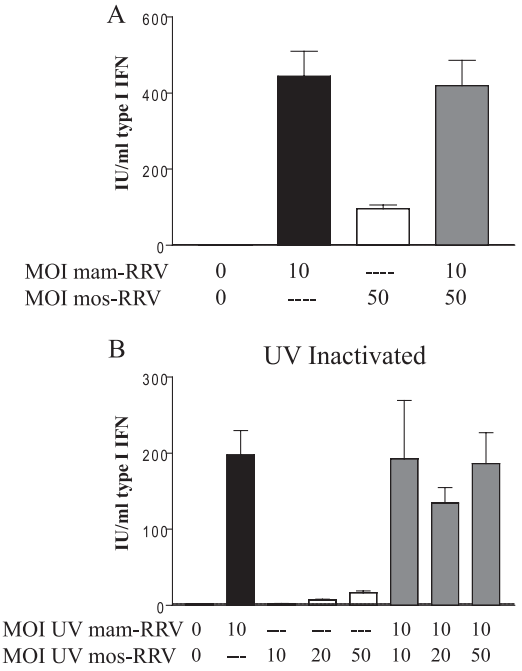

FIG. 1. C6/36 cell-derived RRV (mos-RRV) coinoculated with BHK-21 cell-derived RRV (mam-RRV) does not suppress IFN-α/β induction by mam-RRV in murine mDCs. (A) Wild-type mam-RRV and wild-type mos-RRV were used either alone or in combination to infect mDCs at the indicated MOIs. At 12 hpi, supernatants were harvested and IFN-α/β levels were measured by an IFN-α/β bioassay. Type I IFN levels in mDCs incubated with mam-RRV alone (MOI, 10) and mam-RRV (MOI, 10) plus mos-RRV (MOI, 50) were significantly different ($P < 0.05$) from those in mDCs incubated with mos-RRV alone (MOI, 50), as determined by one-way ANOVA. The results of mam-RRV infection were not significantly different from those of mam-RRV and mos-RRV coinfection. —, absent. (B) UV-irradiated (UV) mam-RRV and mos-RRV were used either alone or in combination to infect mDCs at the indicated MOIs. Supernatants were harvested at 12 hpi as described in the legend to panel A to measure IFN-α/β levels. Each bar represents the mean and standard error of the mean for triplicate samples. Type I IFN levels in DCs incubated with mam-RRV alone (MOI, 10) and mam-RRV (MOI, 10) plus mos-RRV (MOI, 50) were significantly different ($P < 0.05$) from those in DCs incubated with mos-RRV alone (MOIs, 10, 20, and 50), as determined by one-way ANOVA. The data shown are representative of results from at least three independent experiments.

To test if each glycan mutant virus was viable, recombinant viral RNA was in vitro transcribed and BHK-21 cells were transfected with the recombinant transcripts. The specific infectivity of the RNA of each virus was determined by agarose overlay of transfected BHK-21 cells and the counting of plaques from each virus. Each mutant virus produced plaques with efficiency similar to that of wild-type RRV and had specific infectivity values ranging between the wild-type value of 6.40×10^3 and 1.50×10^3 PFU/μg of RNA (data not shown).

To confirm that the mutations introduced into the RRV genome abolished each glycosylation site, Western blot analysis of purified virions using anti-RRV antisera against the RRV envelope glycoproteins was performed. Previous studies with dengue virus demonstrated that the removal of an N-

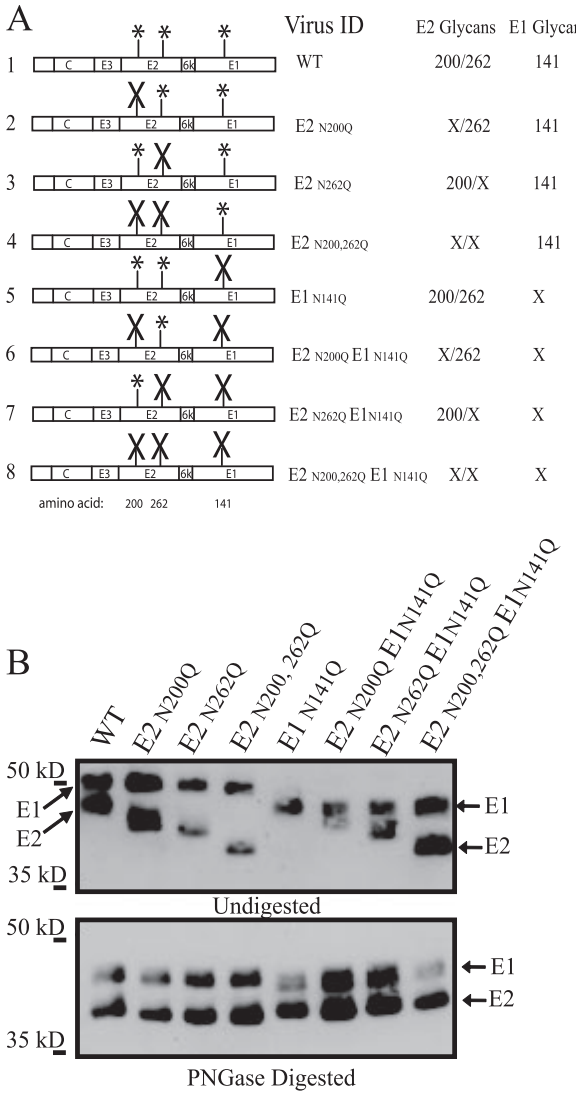

FIG. 2. (A) Diagram of the panel of RRV N-linked glycosylation mutants. The RRV structural proteins are depicted, with the locations of the E2 and E1 N-linked glycosylation sites indicated by asterisks. Each combination of RRV glycan mutations was generated by PCR-site-directed mutagenesis. Mutated sites are indicated by ×'s. Each segment was sequenced and subcloned back into both the pRR64 and the pRR64-GFP plasmid backbones. The numbers to the left of the diagram represent amino acid positions. WT, wild type. (B) RRV mutants missing either a single or a combination of N-linked glycosylation sites on the E2 and E1 glycoproteins are viable. Proteins from purified RRV virions were separated through an SDS–10% PAGE gel, and Western blot analysis of the E2 and E1 proteins was performed with anti-RRV polyclonal antisera. The mutation of each glycosylation site resulted in an approximate 2-kDa reduction in the size of either E1 or E2 (upper panel). The mobility shift of E1 and E2 for each glycan mutant virus corresponds with the predicted shift in molecular mass. The lower panel shows that purified RRV glycan mutants digested with PNGase migrate at approximately the same rates, indicative that migration differences observed in the upper panel are due to the loss of N-linked glycans. Data are representative of results from at least three independent experiments.

linked glycan results in a 2-kDa mobility shift upon SDS-PAGE analysis (32). The upper panel of Fig. 2B depicts differences in the migration of the E1 and E2 glycoproteins between wild-type RRV and each glycan mutant. The elimination of each glycosylation site resulted in a corresponding mobility shift indicative of the loss of each N-linked glycan. The same pattern for the E2 and E1 glycoproteins was also observed with each mos-RRV glycan mutant produced in C6/36 cells (data not shown). PNGase treatment of virions, which removes all N-linked oligosaccharides, indicated that the differences in mobility were due to the loss of one, two, or in the case of the triple mutant, all three oligosaccharides (Fig. 2B, lower panel).

To determine whether the loss of one or more N-linked glycan sites adversely affected viral specific infectivity, we calculated the relative number of RRV genomes per PFU (as determined on BHK-21 cells) by quantitative PCR and established a relative genome/PFU ratio for each virus. Table 1 displays the ratios of genomes to PFU of each mutant mam-RRV as normalized to that for wild-type mam-RRV (therefore, the value for wild-type RRV is set to 1.000). All mam-RRV values were within twofold of one another. We also evaluated the genome/PFU ratio for each RRV glycan mutant derived from mosquito cells. All mos-RRV mutants produced virus particles with genome-to-PFU ratios similar to that for wild-type mos-RRV (Table 1, right two columns). Within both cell lines, no mutant virus had a genome/PFU ratio that differed by more than twofold from the other ratios. In addition, the ratio of the genome-to-PFU ratio for wild-type mos-RRV to that for wild-type mam-RRV was 0.502, which is consistent with the findings of previous studies (29).

To further evaluate if the loss of N-linked glycans impaired RRV replication, we performed single- and multistep growth curve analyses (Fig. 3). The removal of one or both E2 N-linked glycans had little to no effect on viral replication in single- or multistep growth curve analyses (Fig. 3A and C). All RRV glycan mutants missing the E1 amino acid 141 sugar were viable but did exhibit a reduction in viral titers of approximately 1 to 1.5 logs compared to the titer of wild-type RRV in

TABLE 1. Relative numbers of genomes per PFU[a]

Virus	Relative genome no./PFU ratio[b] for variants of:			
	Mam-RRV		Mos-RRV	
	Avg	SEM	Avg	SEM
Wild type	1.000[c]	0.215	1.000[c]	0.033
E2 N200Q	0.643	0.043	0.789	0.047
E2 N262Q	1.232	0.065	0.670	0.054
E2 N200,262Q	0.645	0.051	1.163	0.063
E1 N141Q	1.690	0.077	1.028	0.101
E2 N200Q E1 N141Q	0.628	0.081	0.475	0.022
E2 N262Q E1 N141Q	0.996	0.066	0.647	0.141
E2 N200,262Q E1 N141Q	0.946	0.076	1.873	0.202

[a] Ratios for mam-RRV and mos-RRV mutants were normalized to the ratios for wild-type mam-RRV and mos-RRV, respectively. The number of PFU of each virus on BHK-21 cells was determined, and the data are representative of results from two independent experiments.

[b] Ratios were determined by calculating the number of genomes (by TaqMan real-time PCR) for each PFU on BHK-21 cells. Each value represents the mean and standard error of the mean (SEM) of results for triplicate RNA extractions from each virus preparation.

[c] Each mam-RRV value was normalized to the wild-type mam-RRV genome/PFU ratio, and each mos-RRV value was normalized to the wild-type mos-RRV genome/PFU ratio, with the average wild-type ratio set at 1.000. The ratio of the wild-type mos-RRV ratio to the wild-type mam-RRV ratio in this experiment was 0.502, consistent with previous results (29).

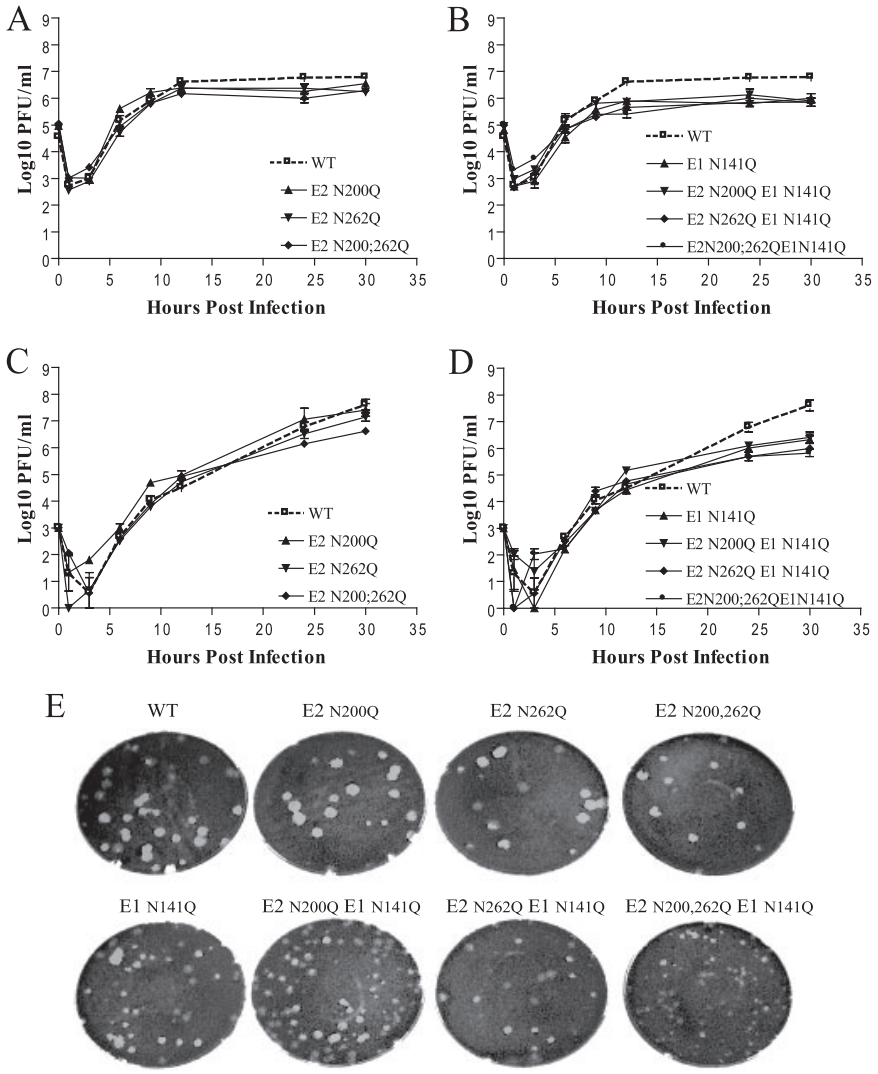

FIG. 3. (A to D) Growth curves from multistep and single-step analyses of wild-type (WT) RRV and RRV glycan mutants on BHK-21 cells. BHK-21 cells were infected with wild-type RRV and each glycan mutant at an MOI of 0.01 (multistep) (A and B) or an MOI of 5 (single step) (C and D) for 1 h. Output titers at 1, 3, 6, 9, 12, 24, and 30 hpi are plotted. Each data point represents the mean and standard error of the mean for three independent samples. (E) Crystal violet plaque assay staining of wild-type and glycoprotein mutant RRVs from separate multistep growth curve analyses at 9 hpi demonstrates differences in plaque morphology between each glycan mutant and wild-type RRV. All data are representative of results from at least three independent experiments.

both single- and multistep growth curve analyses at late times postinfection (Fig. 3B and D). In addition to a slight reduction in the end point titer, RRV missing all three N-linked glycan sites displayed a small-plaque phenotype on BHK-21 cells (Fig. 3E).

Identification of the predominant oligosaccharide at each glycosylation site of mam- and mos-RRV. A major difference between virus particles produced from mammalian cells and virus particles produced from insect cells is that insect cell-derived viruses have only terminal mannose sugars attached to their viral glycoproteins and mammalian-cell-derived viruses may have complex, mannose, or a mixture of both (hybrid) oligosaccharides (13, 14). We utilized the RRV glycan mutant panel to determine the predominant oligosaccharide at each glycosylation site of mam- and mos-RRV. Individual mutants of mam- and mos-RRV were digested with either PNGase F or endo H. PNGase F nonspecifically cleaves all complex, mannose, and hybrid N-linked glycans. Endo H cleaves high-mannose and hybrid sugars but does not cleave paucimannose or complex sugars (33). Following digestion with each endoglycosidase, the glycans on the E2 and E1 glycoproteins were analyzed by Western blotting using anti-RRV antisera (Fig. 4 and Table 2). PNGase and endo H digestion of the mam-RRV mutant E2 N262Q (which had one E2 sugar at amino acid 200) demonstrated that the E2 amino acid 200 sugar was PNGase and endo H sensitive (Fig. 4A, lanes 7 to 9). This result indicated that the predominant oligosaccharide at amino acid 200 was either a hybrid (both complex and high mannose) or high mannose. Mam-RRV also had two PNGase-sensitive, endo H-resistant sugars (at E2 amino acid 262 and E1 amino acid 141), indicating the presence of complex sugars at both of these sites (Fig. 4A, lanes 4 to 6 and 10 to 12).

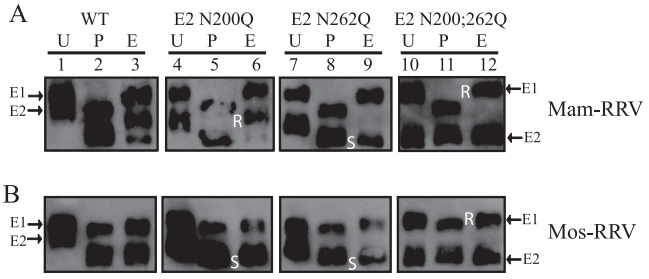

FIG. 4. Identification of the predominant oligosaccharide at each glycosylation site of RRV produced in BHK-21 and C6/36 cells. Wild-type RRV, RRV mutant E2 N200Q, RRV mutant E2 N262Q, and RRV mutant E2 N200,262Q were either undigested (U) or digested with either PNGase (P) or endo H (E) overnight and then analyzed by SDS-PAGE, followed by Western blotting with anti-RRV polyclonal antisera. (A) Analysis of digestions of RRV grown in BHK-21 cells (mam-RRV). (B) Analysis of digestions of RRV grown in C6/36 cells (mos-RRV). The letters R and S on the lower left sides of the E2 and E1 glycoproteins in the endo H lanes indicate if the oligosaccharide on that glycoprotein is endo H resistant (R) or sensitive (S) compared to the corresponding glycoprotein in the uncut (U) lane. Data are representative of results from at least three independent experiments.

Since arthropods do not produce complex glycans (3), the mos-RRV envelope has either high-mannose or paucimannose (3-mannose-residue) oligosaccharides. PNGase and endo H digestion of mos-RRV glycan mutants revealed that both E2 sugars were endo H sensitive, indicative of high-mannose (4- to 9-mannose-residue) sugars at these sites (Fig. 4B, second and third panels from the left). Mos-RRV also had one PNGase-sensitive, endo H-resistant sugar (at E1 amino acid 141), indicative of a paucimannose oligosaccharide (3 mannose residues) (Fig. 4B, far right panel). Based on the greater molecular weight difference between the undigested and PNGase-digested forms of the E1 glycoprotein of mam-RRV than between those of mos-RRV, it is likely that the amino acid 141 sugar is complex in mammalian cells and paucimannose in insect cells (compare the far right panels of Fig. 4A and B). Table 2 summarizes the results in Fig. 4, listing the endo H sensitivity for each N-linked glycan and the predominant oligosaccharide at each site for both mam- and mos-RRV.

The removal of N-linked oligosaccharides on the E2 glycoprotein of mos-RRV reduces the infection efficiency of the virus in murine mDCs but does not affect IFN-α/β production. The coinfection study results presented in Fig. 1 indicated that mos-RRV did not actively inhibit IFN-α/β induction by mam-RRV in mDCs. To assess this issue further, we grew the panel of N-linked glycan mutants in mosquito cells and evaluated these viruses for their ability to induce IFN-α/β. We hypothesized that if high-mannose N-linked glycans on the mosquito cell-derived virus were actively inhibiting IFN-α/β, viruses lacking one or more of these glycosylation sites would permit IFN-α/β induction. As shown in Fig. 5A, wild-type mos-RRV infected more mDCs than wild-type mam-RRV (21% versus 3%). Infection percentages were consistently reduced with mos-RRV lacking all three N-linked glycans (12% of cells were infected), though surprisingly, the removal of all three N-linked glycans did not completely reduce the infection efficiency of the mosquito cell-derived virus to that of wild-type mam-RRV. Most importantly, none of the mosquito cell-derived viruses lacking one, two, or all three N-linked glycans exhibited high-level induction of IFN-α/β (yielding 25 to 50 IU/ml) in mDCs compared to that by mam-RRV (yielding 320 IU/ml) (Fig. 5B), further suggesting that the presence of high-mannose N-linked glycans on mos-RRV does not inhibit IFN-α/β induction in mDCs.

N-linked oligosaccharides on the E2 glycoprotein of mam-RRV are required for robust IFN-α/β induction in mDCs. An alternative to the hypothesis that high-mannose N-linked glycans suppress IFN-α/β is the possibility that complex N-linked glycans on mam-RRV promote IFN-α/β induction in mDCs. Studies with other viruses have demonstrated a role of N-linked glycans on the virus particle in the induction of IFN-α/β in cultured cells (4, 23, 37). Therefore, each glycan mutant virus was grown in BHK-21 cells and evaluated for its ability to infect mDCs and induce IFN-α/β. Wild-type mam-RRV and each envelope glycan mutant infected mDCs to similar levels, between 5 and 7% (Fig. 5C and data not shown); however, while wild-type virus induced IFN-α/β to high levels (1,000 to 1,100 IU/ml), viruses lacking both E2 glycans corresponded to a reduction in IFN-α/β (220 to 240 IU/ml), while the removal of the E1 glycan had no effect on IFN-α/β induction (yielding 1,300 to 1,700 IU/ml) (Fig. 5D). To validate these results, IFN-β and IFN-α ELISAs were performed with the supernatants from the infected cultures characterized in Fig. 5D. Though IFN-α levels were below the limit of detection for the assay, IFN-β levels correlated tightly with the IFN bioassay results (Fig. 5E). The ELISA data both validate the IFN bioassay results and indicate that the majority of the IFN measured in the bioassay is IFN-β.

To ensure that the diminished IFN-α/β induction was not due simply to reduced infection efficiency within the culture, we infected mDCs with wild-type mam-RRV or the mam-RRV mutant designated E2 N200,262Q at a higher MOI of 50 and measured IFN-α/β induction. As shown in Fig. 5F and G, even when a large percentage of mDCs within the culture were infected with both viruses, the E2 glycan-deficient virus still showed reduced IFN-α/β induction compared to the wild-type virus. These results suggest that the failure of mos-RRV to elicit strong IFN-α/β responses in mDCs is due at least partly to a lack of complex N-linked glycans on mos-RRV rather than the active inhibition of IFN-α/β induction by mos-RRV.

TABLE 2. Identification of the predominant oligosaccharide type at each N-linked glycosylation site in BHK-21 and C6/36 cells

Virus and glycosylation site	Endo H sensitivity	Predominant oligosaccharide type(s)
Mam-RRV		
E2 amino acid 200	Sensitive	High mannose/hybrid
E2 amino acid 262	Resistant	Complex
E1 amino acid 141	Resistant	Complex
Mos-RRV		
E2 amino acid 200	Sensitive	High mannose
E2 amino acid 262	Sensitive	High mannose
E1 amino acid 141	Resistant	Paucimannose

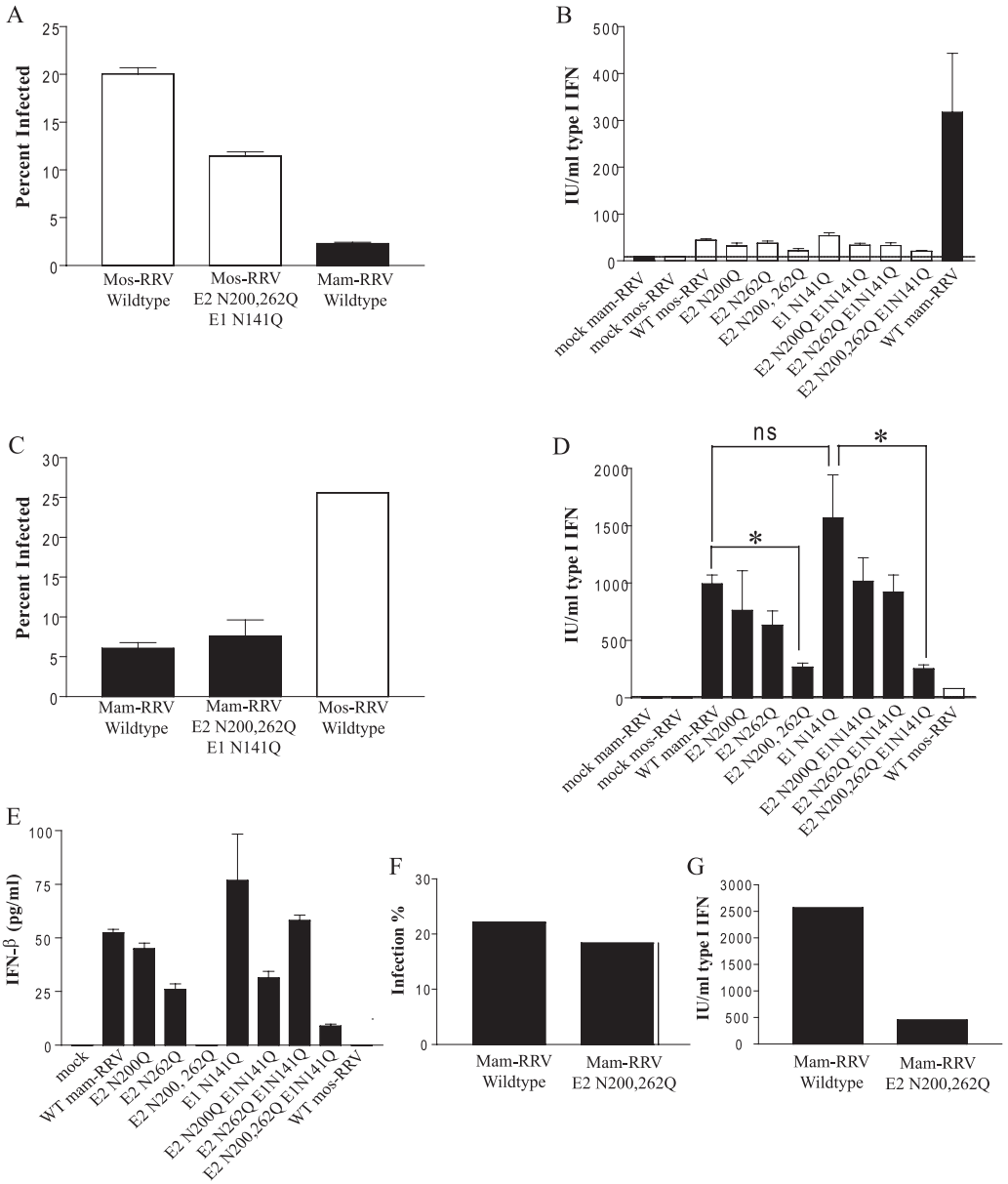

FIG. 5. The robust IFN-α/β induction by BHK-21 cell-derived RRV (mam-RRV) on DCs correlates with the presence of the E2 N-linked glycans on the virus particle. (A) Percentages of mDCs infected with wild-type mos-RRV, mos-RRV mutant E2 N200,262Q E1 N141Q, and wild-type mam-RRV at an MOI of 10. Infection was quantified by fluorescence-activated cell sorting and the counting of GFP-positive cells at 12 hpi. The results represented by each bar are significantly different from those represented by each other bar as determined by one-way ANOVA. (B) Levels of type I IFN produced in the samples described in the legend to panel A and in samples of mDCs infected with each RRV glycan mutant grown in C6/36 cells. Murine mDCs were infected at an MOI of 10, and at 12 hpi, supernatants were harvested for an IFN-α/β bioassay. Each bar represents the mean and standard error of the mean for triplicate samples. The level of type I IFN induced by mam-RRV was significantly different from that induced by each mos-RRV mutant virus as determined by one-way ANOVA. WT, wild type. (C) Percentages of mDCs infected with wild-type mam-RRV, mam-RRV mutant E2 N200,262Q E1 N141Q, and wild-type mos-RRV at an MOI of 20. Each mam-RRV bar represents the mean and standard error of the mean for triplicate samples, while the mos-RRV bar represents the mean for duplicate samples. Infectivity differences between mos-RRV and mam-RRV and between mos-RRV and mam-RRV E2 N200,262Q E1 N141Q are statistically significant as determined by one-way ANOVA. (D) Levels of type I IFN produced in the samples described in the legend to panel C and in samples of mDCs infected with each individual glycan mutant virus produced in BHK-21 cells. Each N-linked glycan mutant of mam-RRV was used to infect mDC cultures at an MOI of 20. At 12 hpi, supernatants were harvested for an IFN-α/β bioassay. Asterisks indicate that the difference between the results for two groups is statistically significant by an unpaired Student *t* test (*, $P < 0.01$). ns indicates that the results for two groups are not significantly different from each other. (E) Results of an ELISA measuring IFN-β production in the cultures of supernatants from the samples described in the legend to panel D. (F) Wild-type mam-RRV and mam-RRV mutant E2 N200,262Q were used to infect mDCs at an MOI of 50 for 12 h; (G) supernatants were analyzed by an IFN-α/β bioassay. Each bar in panels A through E represents the mean and standard error of the mean for triplicate samples, except those for mos-RRV in panels C, D, and E, which are representative of results for duplicate samples. Each bar in panels F and G represents the results for a single sample. All data are representative of results from at least three independent experiments.

DISCUSSION

Understanding how alphaviruses cause disease is essential for designing successful strategies for therapeutics and vaccines. One important step in the disease process is the transmission of the virus from the mosquito vector to the vertebrate host, which often involves virus-DC interactions (20, 21, 36). Therefore, we have focused on viral interactions with mDCs and have demonstrated previously that mos-RRV more efficiently infects yet induces less IFN-α/β in these cells than mam-RRV. Studies presented here further dissected the role of N-linked glycans in these early virus-host interactions and demonstrated that complex glycans on the E2 envelope protein of mam-RRV are required for robust IFN-α/β induction (Fig. 5D).

The previously observed lack of high-level IFN-α/β induction by mosquito cell-derived alphaviruses suggested that these viruses are either actively suppressing IFN-α/β induction or are not as potent inducers of IFN-α/β as the mammalian-cell-derived viruses. Arjona et al. recently demonstrated that C6/36-derived WNV can actively suppress murine macrophage activation following stimulation with double-stranded RNA and that the suppression is dependent on high-mannose N-linked glycans (1). In our system, mos-RRV was unable to actively suppress the IFN-α/β induced by mam-RRV infection of mDCs (Fig. 1). Furthermore, a mos-RRV mutant lacking N-linked glycans was still a poor inducer of IFN-α/β, indicating that high-mannose sugars on mos-RRV did not suppress the ability of the DCs to respond to viral infection. Instead, our results suggest that the presence of complex N-linked sugars on the E2 glycoprotein of mam-RRV leads to enhanced IFN-α/β induction and that mos-RRV is a poor inducer due, at least in part, to its lack of complex N-linked glycans. Furthermore, our results demonstrate that the complex sugar on the E1 glycoprotein of mam-RRV does not play a role in IFN-α/β induction, since mam-RRV mutant E1 N141Q induced levels of IFN-α/β equivalent to those induced by wild-type mam-RRV (Fig. 5D). However, all mutants lacking E1 glycosylation displayed minor but similar growth defects in BHK-21 cells (Fig. 3), suggesting that E1 amino acid 141 is required for optimal virus particle production but not for IFN-α/β induction in mDCs. Based on the Sindbis alphavirus structure (25), E1 potentially lies below the E2 glycoprotein on the surface of the virion. Therefore, E1 may not contact the cellular receptor/sensing molecule responsible for inducing IFN-α/β; however, this idea requires further investigation since the arrangement of the RRV glycoproteins may differ from that of the Sindbis virus glycoproteins.

Our data are consistent with the findings of several studies which have demonstrated that viral glycosylation can promote IFN-α/β induction (2, 6, 19, 23, 38) and that complex but not high-mannose N-linked glycans are responsible for IFN-α/β induction (4). However, it is certainly possible that mosquito cell-derived alphaviruses actively suppress IFN-α/β induction but that we were unable to detect this effect or that different results in other cell types, such as macrophages or human DCs, may be observed. For example, C6/36-derived WNV actively suppresses receptor-interacting protein 1 (RIP-1) signaling in murine macrophages (1). Additional reports demonstrated that the level of IFN-α/β produced in plasmacytoid DCs infected with C7/10-cell derived WNV is drastically reduced compared to that produced in cells infected with Vero cell-derived WNV but that C7/10-cell derived WNV is not able to actively inhibit IFN-α/β induction by Sendai virus (31).

Our results strongly suggest that viral complex/hybrid N-linked glycans promote IFN-α/β responses in mDCs, which implicates a couple of potential mechanisms underlying this process. Though the mos-RRV and mam-RRV target the same CD11c-positive cell populations in the mDC cultures (data not shown), differential interactions with lectin receptors on the surfaces of mDCs may direct the mosquito and mammalian-cell-derived viruses to different compartments within the mDC. For example, the mammalian-cell-derived virus may enter the mDC differently from the mosquito cell-derived virus, thereby causing the viral RNA to come into contact with host sensor molecules, such as Toll-like receptors (TLRs) or RIG-I, with greater efficiency than the mos-RRV. Alternatively, several groups have shown that viral glycosylation plays a positive role in driving IFN-α/β responses (2, 6, 19, 23, 38). Therefore, lectin receptors on mDCs may be triggered by the glycans of mam-RRV, but not those of mos-RRV, to enhance IFN-α/β induction through an undefined costimulatory molecule to upregulate the IFN-α/β response. Finally, IFN-α/β induction may be independent of lectin receptors. For example, a pattern recognition molecule, such as a TLR, may also recognize the mam-RRV but not the mos-RRV envelope. Complex glycans arranged in the compact and highly ordered structure of a virus particle can be recognized by the host cell as foreign (40), and TLR-4 can recognize viral glycoproteins and trigger signaling pathways, leading to IFN-α/β production independent of the adaptor MyD88 (9, 11, 18, 26). It is therefore possible that envelope glycosylation patterns on mam-RRV, but not mos-RRV, trigger a CLR, TLR-4, or another cellular protein to induce IFN-α/β following interaction with mDCs. It will also be important to determine whether these N-linked glycan-specific effects are specific to RRV or represent a more general trait of alphaviruses. We have previously shown that mosquito-derived Venezuelan equine encephalitis virus and Barmah Forest virus (BFV) are poor IFN-α/β inducers compared to mammal-derived viruses (29), suggesting that a similar role for complex N-linked glycans of other alphaviruses in driving IFN-α/β induction may exist. However, while the abolishment of the two N-linked glycosylation sites on RRV led to decreased IFN-α/β induction, a BFV variant lacking N-linked glycans on the E2 glycoprotein was a robust inducer of type I IFN mRNA when the virus was derived from either mammalian or mosquito cells (29). This result raises the possibility that BFV may differ from RRV, as the presence of high-mannose N-linked glycans on the E2 glycoprotein of BFV may actively suppress IFN-α/β induction. However, this possibility requires further investigation.

In addition to allowing the dissection of viral glycosylation in regulating IFN-α/β induction by mosquito and mammalian-cell-derived viruses, the generation of this panel of RRV mutants provided a useful set of tools for identifying the predominant type of glycosylation at each N-linked site and for assessing the relative contribution of each N-linked glycan site in mediating the enhanced infection of mDCs by mos-RRV. A similar panel of glycan mutants of Sindbis virus demonstrated that the elimination of two or more N-linked glycosylation sites

causes severe growth restriction (25). In the present study, RRV glycan mutants were viable and displayed some growth defects but were not as severely impaired in particle production as the Sindbis virus mutants.

As expected, endo H digestions verified that the mos-RRV envelope contains both high-mannose and paucimannose oligosaccharides. In contrast, mam-RRV has two complex sugars as the predominant form at the E1 amino acid 141 and E2 amino acid 262 glycosylation sites, while the E2 amino acid 200 glycosylation site contains hybrid sugars (both mannose and complex sugars) and/or high-mannose sugars (Fig. 4). The presence of an endo H-sensitive sugar on the E2 protein of mam-RRV is due likely to the masking of the E2 amino acid 200 site by E1 or the immature precursor of E2 (PE2) to prevent complete carbohydrate processing during glycoprotein assembly in the endoplasmic reticulum and Golgi system (27, 34). Incomplete glycan processing also occurs with Sindbis virus glycoproteins (14), and it would be interesting to determine whether this effect has any impact on IFN-α/β induction. Finally, though we observed decreased infection efficiency in mDCs when all three N-linked glycosylation sites were removed from mos-RRV, which is consistent with previous findings that demonstrated a role for high-mannose N-linked glycans in promoting enhanced infection by mosquito-derived alphaviruses, the triple mutant virus still infected mDCs to a higher level than mam-RRV. One interpretation of these results may be that factors other than glycosylation influence the enhanced infection of mDCs by mosquito-derived alphaviruses; however, additional analysis of these RRV mutants and other alphaviruses is required before this conclusion can truly be made. Our analysis clearly shows that the mutation of all three N-linked glycosylation sites removed all N-linked glycans from the virus (Fig. 2B). Furthermore, when these mutant viruses were derived from mammalian cells, they were as infectious for mDCs as wild-type mam-RRV (Fig. 5); however, we cannot rule out the possibility that one or more of the mutations subtly altered viral folding when virus was grown in mosquito cells and that a slightly changed viral conformation was responsible for the enhanced mDC infection by the triple mutant mos-RRV. Therefore, not only will these results need to be confirmed with other alphaviruses, but other techniques, such as the digestion of the virion with glycosidases, should be used to further assess whether mosquito-derived alphaviruses exhibit enhanced infection efficiency for mDCs in a glycan-independent manner.

In summary, we have found that N-linked glycans on the E2 glycoprotein of mam-RRV are required for robust IFN-α/β responses against RRV. This finding suggests that mosquito cell-derived alphaviruses may avoid the induction of IFN-α/β due simply to their lack of complex N-linked oligosaccharides on the virion rather than the active inhibition of IFN-α/β production. Additional studies are under way to determine whether this effect is common to multiple alphaviruses and to define the mechanism underlying the role of complex N-linked glycans in promoting virus-induced IFN-α/β responses.

ACKNOWLEDGMENTS

We thank Nancy Davis, Tem Morrison, Clayton Beard, Cathy Cruz, Jason Simmons, Amy Wollish, Kari Hacker, and Robert Johnston for helpful scientific discussions and/or critical readings of the manuscript. We thank Bianca Trollinger for assistance with cell culture.

The work was supported by research grant number 5R21AI064645-02, awarded to M.T.H. R.S.S. was supported by a UNC virology training grant and a UNC dissertation completion fellowship.

REFERENCES

1. **Arjona, A., M. Ledizet, K. Anthony, N. Bonafe, Y. Modis, T. Town, and E. Fikrig.** 2007. West Nile virus envelope protein inhibits dsRNA-induced innate immune responses. J. Immunol. **179:**8403–8409.
2. **Baudoux, P., C. Carrat, L. Besnardeau, B. Charley, and H. Laude.** 1998. Coronavirus pseudoparticles formed with recombinant M and E proteins induce alpha interferon synthesis by leukocytes. J. Virol. **72:**8636–8643.
3. **Butters, T. D., R. C. Hughes, and P. Vischer.** 1981. Steps in the biosynthesis of mosquito cell membrane glycoproteins and the effects of tunicamycin. Biochim. Biophys. Acta **640:**672–686.
4. **Charley, B., L. Lavenant, and B. Delmas.** 1991. Glycosylation is required for coronavirus TGEV to induce an efficient production of IFN alpha by blood mononuclear cells. Scand. J. Immunol. **33:**435–440.
5. **Davis, C. W., H.-Y. Nguyen, S. L. Hanna, M. D. Sanchez, R. W. Doms, and T. C. Pierson.** 2006. West Nile virus discriminates between DC-SIGN and DC-SIGNR for cellular attachment and infection. J. Virol. **80:**1290–1301.
6. **de Haan, C. A., M. de Wit, L. Kuo, C. Montalto-Morrison, B. L. Haagmans, S. R. Weiss, P. S. Masters, and P. J. Rottier.** 2003. The glycosylation status of the murine hepatitis coronavirus M protein affects the interferogenic capacity of the virus in vitro and its ability to replicate in the liver but not the brain. Virology **312:**395–406.
7. **Diebold, S. S., M. Montoya, H. Unger, L. Alexopoulou, P. Roy, L. E. Haswell, A. Al-Shamkhani, R. Flavell, P. Borrow, and C. Reis e Sousa.** 2003. Viral infection switches non-plasmacytoid dendritic cells into high interferon producers. Nature **424:**324–328.
8. **Enserink, M.** 2007. Infectious diseases. Chikungunya: no longer a Third World disease. Science **318:**1860–1861. doi:10.1126/science.318.5858.1860.
9. **Georgel, P., Z. Jiang, S. Kunz, E. Janssen, J. Mols, K. Hoebe, S. Bahram, M. B. A. Oldstone, and B. Beutler.** 2007. Vesicular stomatitis virus glycoprotein G activates a specific antiviral Toll-like receptor 4-dependent pathway. Virology **362:**304–313.
10. **Hidmark, A. S., G. M. McInerney, E. K. L. Nordstrom, I. Douagi, K. M. Werner, P. Liljestrom, and G. B. K. Hedestam.** 2005. Early alpha/beta interferon production by myeloid dendritic cells in response to UV-inactivated virus requires viral entry and interferon regulatory factor 3 but not MyD88. J. Virol. **79:**10376–10385.
11. **Hoebe, K., X. Du, P. Georgel, E. Janssen, K. Tabeta, S. O. Kim, J. Goode, P. Lin, N. Mann, S. Mudd, K. Crozat, S. Sovath, J. Han, and B. Beutler.** 2003. Identification of Lps2 as a key transducer of MyD88-independent TIR signalling. Nature **424:**743–748.
12. **Holbrook, M. R., and B. B. Gowen.** 2008. Animal models of highly pathogenic RNA viral infections: encephalitis viruses. Antivir. Res. **78:**69–78.
13. **Hsieh, P., and P. W. Robbins.** 1984. Regulation of asparagine-linked oligosaccharide processing. Oligosaccharide processing in Aedes albopictus mosquito cells. J. Biol. Chem. **259:**2375–2382.
14. **Hsieh, P., M. R. Rosner, and P. W. Robbins.** 1983. Host-dependent variation of asparagine-linked oligosaccharides at individual glycosylation sites of Sindbis virus glycoproteins. J. Biol. Chem. **258:**2548–2554.
15. **Ito, Y.** 1994. Induction of interferon by virus glycoprotein(s) in lymphoid cells through interaction with the cellular receptors via lectin-like action: an alternative interferon induction mechanism. Arch. Virol. **138:**187–198.
16. **Klimstra, W. B., E. M. Nangle, M. S. Smith, A. D. Yurochko, and K. D. Ryman.** 2003. DC-SIGN and L-SIGN can act as attachment receptors for alphaviruses and distinguish between mosquito cell- and mammalian cell-derived viruses. J. Virol. **77:**12022–12032.
17. **Kuhn, R. J., H. G. Niesters, Z. Hong, and J. H. Strauss.** 1991. Infectious RNA transcripts from Ross River virus cDNA clones and the construction and characterization of defined chimeras with Sindbis virus. Virology **182:** 430–441.
18. **Kurt-Jones, E. A., L. Popova, L. Kwinn, L. M. Haynes, L. P. Jones, R. A. Tripp, E. E. Walsh, M. W. Freeman, D. T. Golenbock, L. J. Anderson, and R. W. Finberg.** 2000. Pattern recognition receptors TLR4 and CD14 mediate response to respiratory syncytial virus. Nat. Immunol. **1:**398–401.
19. **Laude, H., J. Gelfi, L. Lavenant, and B. Charley.** 1992. Single amino acid changes in the viral glycoprotein M affect induction of alpha interferon by the coronavirus transmissible gastroenteritis virus. J. Virol. **66:**743–749.
20. **Libraty, D. H., S. Pichyangkul, C. Ajariyakhajorn, T. P. Endy, and F. A. Ennis.** 2001. Human dendritic cells are activated by dengue virus infection: enhancement by gamma interferon and implications for disease pathogenesis. J. Virol. **75:**3501–3508.
21. **MacDonald, G. H., and R. E. Johnston.** 2000. Role of dendritic cell targeting in Venezuelan equine encephalitis virus pathogenesis. J. Virol. **74:**914–922.
22. **Martinez, O., C. Valmas, and C. F. Basler.** 2007. Ebola virus-like particle-induced activation of NF-κB and Erk signaling in human dendritic cells requires the glycoprotein mucin domain. Virology **364:**342–354.

23. **Miller, J. L., and E. M. Anders.** 2003. Virus-cell interactions in the induction of type 1 interferon by influenza virus in mouse spleen cells. J. Gen. Virol. **84:**193–202.
24. **Mukhopadhyay, S., R. J. Kuhn, and M. G. Rossmann.** 2005. A structural perspective of the flavivirus life cycle. Nat. Rev. Microbiol. **3:**13–22.
25. **Pletnev, S. V., W. Zhang, S. Mukhopadhyay, B. R. Fisher, R. Hernandez, D. T. Brown, T. S. Baker, M. G. Rossmann, and R. J. Kuhn.** 2001. Locations of carbohydrate sites on alphavirus glycoproteins show that E1 forms an icosahedral scaffold. Cell **105:**127–136.
26. **Rassa, J. C., J. L. Meyers, Y. Zhang, R. Kudaravalli, and S. R. Ross.** 2002. Murine retroviruses activate B cells via interaction with toll-like receptor 4. Proc. Natl. Acad. Sci. USA **99:**2281–2286. doi:10.1073/pnas.042355399.
27. **Sariola, M., J. Saraste, and E. Kuismanen.** 1995. Communication of post-Golgi elements with early endocytic pathway: regulation of endoproteolytic cleavage of Semliki Forest virus p62 precursor. J. Cell Sci. **108:**2465–2475.
28. **Serody, J. S., E. J. Collins II, R. M. Tisch, J. J. Kuhns, and J. A. Frelinger.** 2000. T cell activity after dendritic cell vaccination is dependent on both the type of antigen and the mode of delivery. J. Immunol. **164:**4961–4967.
29. **Shabman, R. S., T. E. Morrison, C. Moore, L. White, M. S. Suthar, L. Hueston, N. Rulli, B. Lidbury, J. P. Ting, S. Mahalingam, and M. T. Heise.** 2007. Differential induction of type I interferon responses in myeloid dendritic cells by mosquito and mammalian-cell-derived alphaviruses. J. Virol. **81:**237–247.
30. **Shan, M., P. J. Klasse, K. Banerjee, A. K. Dey, S. P. N. Iyer, R. Dionisio, D. Charles, L. Campbell-Gardener, W. C. Olson, R. W. Sanders, and J. P. Moore.** 2007. HIV-1 gp120 mannoses induce immunosuppressive responses from dendritic cells. PLoS Pathog. **3:**e169.
31. **Silva, M. C., A. Guerrero-Plata, F. D. Gilfoy, R. P. Garofalo, and P. W. Mason.** 2007. Differential activation of human monocyte-derived and plasmacytoid dendritic cells by West Nile virus generated in different host cells. J. Virol. **81:**13640–13648.
32. **Smith, G. W., and P. J. Wright.** 1985. Synthesis of proteins and glycoproteins in dengue type 2 virus-infected Vero and Aedes albopictus cells. J. Gen. Virol. **66:**559–571.
33. **Tarentino, A. L., R. B. Trimble, and T. H. Plummer, Jr.** 1989. Enzymatic approaches for studying the structure, synthesis, and processing of glycoproteins. Methods Cell Biol. **32:**111–139.
34. **Watson, D. G., J. M. Moehring, and T. J. Moehring.** 1991. A mutant CHO-K1 strain with resistance to *Pseudomonas* exotoxin A and alphaviruses fails to cleave Sindbis virus glycoprotein PE2. J. Virol. **65:**2332–2339.
35. **White, L. J., J.-G. Wang, N. L. Davis, and R. E. Johnston.** 2001. Role of alpha/beta interferon in Venezuelan equine encephalitis virus pathogenesis: effect of an attenuating mutation in the 5′ untranslated region. J. Virol. **75:**3706–3718.
36. **Wu, S.-J. L., G. Grouard-Vogel, W. Sun, J. R. Mascola, E. Brachtel, R. Putvatana, M. K. Louder, L. Filgueira, M. A. Marovich, H. K. Wong, A. Blauvelt, G. S. Murphy, M. L. Robb, B. L. Innes, D. L. Birx, C. G. Hayes, and S. S. Frankel.** 2000. Human skin Langerhans cells are targets of dengue virus infection. Nat. Med. **6:**816–820.
37. **Zeng, J., P. Fournier, and V. Schirrmacher.** 2002. Induction of interferon-α and tumor necrosis factor-related apoptosis-inducing ligand in human blood mononuclear cells by hemagglutinin-neuraminidase but not F protein of Newcastle disease virus. Virology **297:**19–30.
38. **Zeng, J., P. Fournier, and V. Schirrmacher.** 2002. Stimulation of human natural interferon-alpha response via paramyxovirus hemagglutinin lectin-cell interaction. J. Mol. Med. **80:**443–451.
39. **Zhang, W., M. Heil, R. J. Kuhn, and T. S. Baker.** 2005. Heparin binding sites on Ross River virus revealed by electron cryo-microscopy. Virology **332:**511–518.
40. **Zinkernagel, R.** 1996. Immunology taught by viruses. Science **271:**173–178.